Effect of Short-Crestedness on Wave Loads on Caisson

Frigaard, Peter Bak; Helm-Petersen, J.; Christensen, M.; Burcharth, Hans Falk

Published in:
Proceedings of the Final Project Workshop

Publication date:
1995

Document Version
Early version, also known as pre-print

Caisson Investigations

Combined LIP–MAST–TAW Project

Effects of short–crestedness on wave loads on caissons

Report by

Peter Frigaard
Jacob Helm–Petersen
Morten Christensen
Hans F. Burcharth

April 1995

Hydraulics & Coastal Engineering Laboratory
Department of Civil Engineering
Aalborg University
Sohngaardsholmsvej 57, DK–9000 Aalborg

Contents

1 Introduction

This report concerns experiments carried out as a combined LIP–MAST–TAW project during May to July, 1994, in the Vinje–Basin at Delft Hydraulics.

Experiments were carried out in order to investigate the performance of caisson breakwaters exposed to irregular multidirectional seas.

The present report is focusing on maximum total wave forces on the caissons as a function of the length of the caissons.

In order to calculate the wave forces from the incident waves a new method being able to calculate wave forces in real time is described.

2 Experimental Setup

2.1 Physical Model

A scale model of a caisson breakwater was designed and constructed in plywood.

The model consisted of thirteen individual caissons, each having a width of 0.9 m and two roundheads covered with a thin steel shell, see figure 4. The model was placed on a permeable two layer berm. Other relevant dimensions are shown in figure 1, which shows a cross–section of the model.

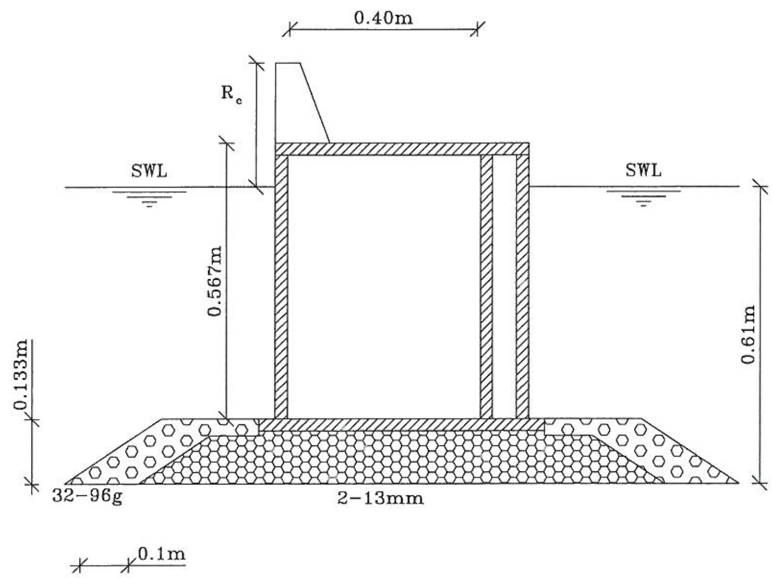

Figure 1: Cross–section of caisson and foundation berm.

As indicated on figure 1 the caissons were constructed with a crest. The crest was replaceable in order to vary the crest height R_c. Further it was the idea to use two different crest heights simultaneously, i.e. the first 7 caissons having one crest height and the remaining 6 caissons another crest height. It is assumed, that the various types of crests did not have any significant influence on the reflection characteristics and the homogeneity of the wave fields in the area covered by the wave gauges.

Four different types of caissons were constructed. These are listed below.

- Caissons with plain vertical front.
- Caissons with impermeable berm (berm level just below SWL).
- Caissons with impermeable slope 1:3 and top just below SWL.
- Caissons with perforated vertical front.

The impermeable berm and the slope were constructed in concrete. Figure 2 shows the geometries.

Two permeable fronts were prepared for the caissons. The design of the permeable fronts are shown in figure 3. The porosity of each type was approximately 25%.

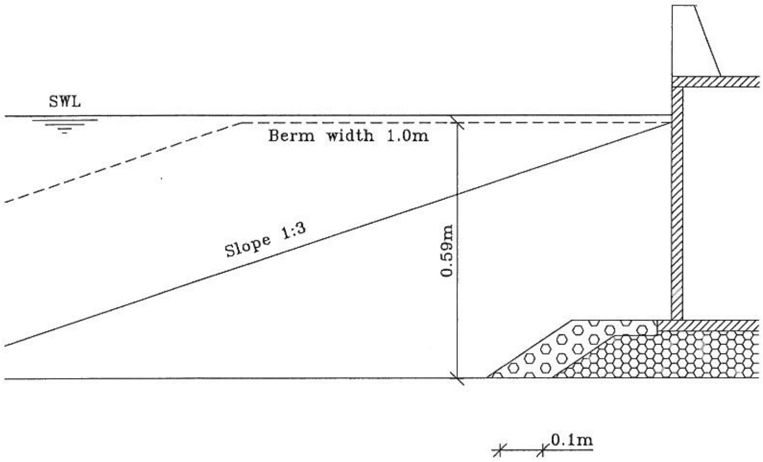

Figure 2: Cross–section of caisson with berm and front slope.

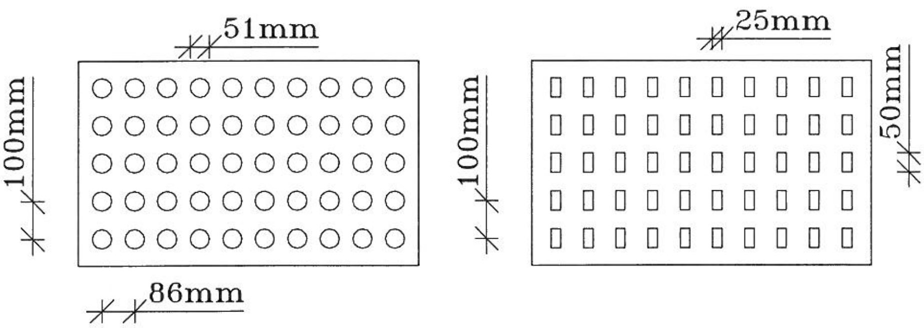

Figure 3: Geometries of permeable fronts.

2.2 Wave Basin

The model was prepared for experiments in the Vinje–Basin at Delft Hydraulics, The Netherlands.

The basin is a multidirectional wave basin capable of generating irregular multidirectional waves with a significant wave height up to about 0.15 m at a water depth of 0.61 m.

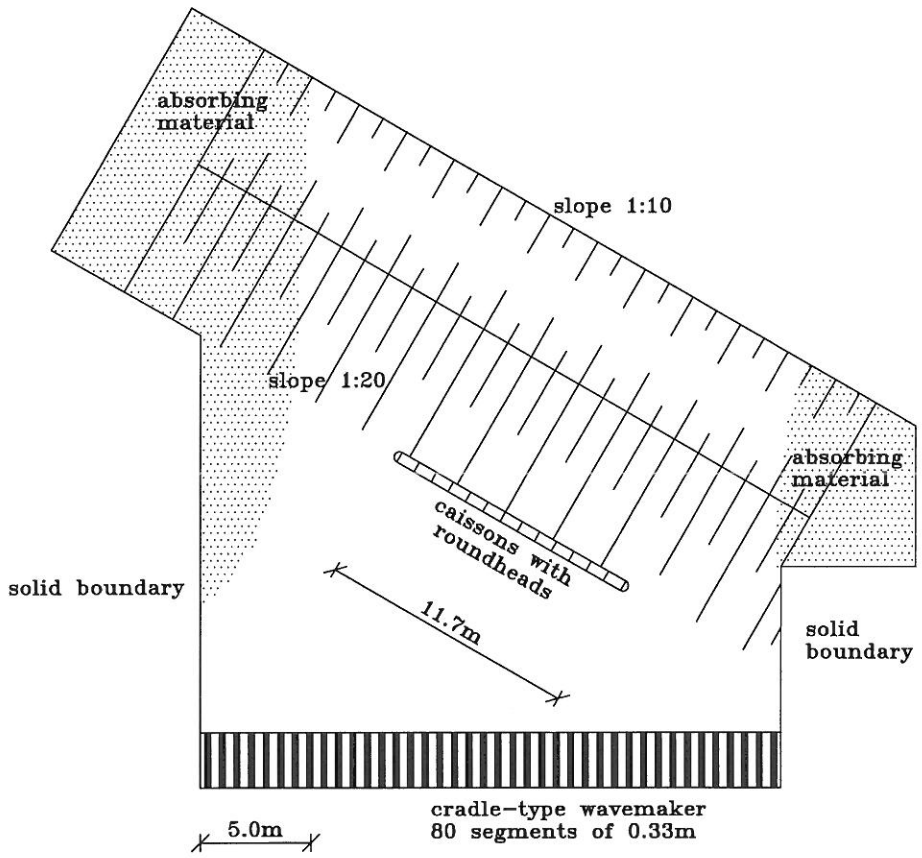

Figure 4: Position of model in the Vinje–Basin at Delft Hydraulics.

In order to provide an acceptable absorption of the waves at the rear boundary the basin has been equipped with a straight sloping foreshore.

Due to the high reflection from the caissons, especially for those with a plain front, various absorbing material were placed in the basin during the tests in order to avoid an unacceptable amount of re–reflection at the solid boundaries and at the wavepaddles. Absorbing material were placed at the side boundaries and at the roundheads. The absorbing material was rearranged for the most oblique waves.

The water depth during all tests was 0.61 m in the area between the caissons and the wavepaddles.

2.3 Instrumentation

The model was equipped, such that it was possible to measure the total forces on the center caisson, the accumulated overtopping at two distinct positions, the number of overtopping waves at the same two positions, the pressure distribution on the fronts (vertical and horizontal) and the pressure distribution below the caissons. Further an array of 20 linear resistance wave gauges were placed in front of the caissons.

The wave gauges were placed in a 0.5×0.5 m grid. Two lines with 10 gauges were placed on a beam supported at each end on two legs having a diameter of approx. 15 mm. The stability of the beams appeared to be satisfactory during the tests. The array of wave gauges was placed as shown on figure 5.

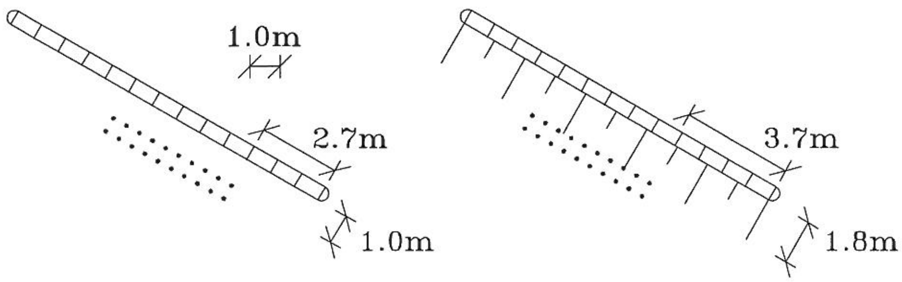

Figure 5: Positioning of wave gauges. For caissons with berm the array was placed with the first line of gauges (closest to the caissons) just above the toe of the berm.

3 Test Conditions

3.1 Incident Wave Field

Target specifications for the incident waves are listed in table 1.

Wave spectrum	JONSWAP
Peak period, T_p	$1.5s$
Significant wave height, H_{s_I}	$0.14m$
Wave steepness H_{s0}/L_{0p}	0.04
Main direction, θ_M	$90°$, $80°$, $70°$, $50°$ or $30°$
Type of spreading	Gaussian
Standard deviation of spreading, σ	$0°, 15°$ or $30°$

Table 1: Incident wave conditions.

All wave conditions were with irregular non–breaking waves. Most of the tests were performed with short crested waves.

3.2 Test Programme

Test		Vertical			Berm		Vertical	
θ_M	σ	plain front			$0\ m$	$1\ m$	perf. front	
90	0	002	203	302	402	502	602	702
90	15		204					
90	30	005	205	305	405	505	605	705
80	15		213					
70	0	009		309	409	509	609	709
70	15	007	202	307	407	507	607	707
70	30	010		310	410	510	610	710
50	15		201					
50	30	015		315	415	515	615	715
30	0		210					
30	15	017					618	718

Table 2: Test programme. Angles are measured in degrees, where 90° is head–on, and positive is measured clockwise.

Each test was assigned a testnumber referring to the test programme listed in table 2. As it appears from the table, 7 test series were carried out. The conditions for each test series are listed in table 3. Thus the first digit in a testnumber specifies the test series. The remainder is a serial number referring to the testprogramme.

Test series	Front type	R_c/H_{s_I}	
		a	b
0	Vertical plain	1.18	1.63
2	Vertical plain	1.18*	1.18
3	Vertical plain	1.5	1.18*
4	Berm, crest width $0m$	1.5	1.18
5	Berm, crest width $1m$	1.5	1.18
6	Circular perforated	1.5	1.18
7	Rectangular perforated	1.5	1.18

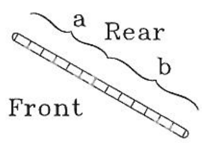

Table 3: Conditions in the 7 test series. Suffix a refers to the left half of caissons and b to the right half. * indicates that the crests were supplied with a nose.

In the following the measured forces and the pressures from test series 0 will be compared with the predicted forces from a real time *force predicter.*

Finally, the effects of short–crestedness on the wave loads on long caissons will be discussed.

4 The Pressure Predicter

The surface elevation at a given point $\overline{x} = (x, y)$ in a irregular directional wave field is given (double summation model) by:

$$\eta(\overline{x}, t) = \sum_{i=1}^{I} \sum_{j=1}^{J} a_{ij} cos(\omega_i t - \overline{k}_{ij} \overline{x} + \phi_{ij}) \tag{1}$$

In the following a method to predict a surface elevation time series (or pressure time series or force timeseries) in a given point $\overline{x}$ from surface elevations measured in the points $\overline{x}_p$, $p = 1, 2, .., P$ in the wave field is developed.

Origo is placed in such a way that $\overline{x} = \overline{0}$. The sought time series will be given by:

$$\eta(t) = \sum_{i=1}^{I} \sum_{j=1}^{J} a_{ij} cos(\omega_i t + \phi_{ij}) \tag{2}$$

The method is digital filtering of the P measured surface elevations through Q linear filters each characterised by a gain $G_{pq}(\omega_i)$ and a phaseshift $\Phi_{pq}(\omega_i)$. The sum of the outputs from these $P \cdot Q$ filters is an estimate on the surface elevation in $\overline{x} = \overline{0}$. The estimate η^* is given by:

$$\eta^*(t) = \sum_{p=1}^{P} \sum_{q=1}^{Q} \sum_{i=1}^{I} \sum_{j=1}^{J} G_{pq}(\omega_i) a_{ij} cos(\omega_i t - \overline{k}_{ij} \overline{x}_p + \phi_{ij} + \Phi_{pq}(\omega_i)) \tag{3}$$

If $G_{pq}(\omega_i) = \frac{1}{P}$ and $\Phi_{pq}(\omega_i) = \overline{k}_q \overline{x}_p$, η^* is calculated from a superposition of Q bandpass filters.

The idea is that each filter q, $q = 1..Q$ corresponds to a specific direction of the waves (given by the wave number vector $\overline{k}_q$), and only waves in that direction will contribute to the sum. The result of the summation will be zero (ideal situation) for waves from all other directions than the direction the filters are created to band-pass.

Filters are created for all directions of incident waves. No filters are created for directions of reflected waves.

If the P measured surface elevations are filtered through Q linear filters each characterised by gain $H_{pq}(\omega_i)$ and phaseshift $\Phi_{pq}(\omega_i)$. Then the sum of the outputs from these $P \cdot Q$ filters is an estimate on the pressure in $\overline{x} = \overline{0}$, p^*:

$$p^*(t) = \sum_{p=1}^{P}\sum_{q=1}^{Q}\sum_{i=1}^{I}\sum_{j=1}^{J} H_{pq}(\omega_i) a_{ij} cos(\omega_i t - \overline{k}_{ij}\overline{x}_p + \phi_{ij} + \Phi_{pq}(\omega_i)) \tag{4}$$

given that $H_{pq}(\omega_i) = \frac{\beta^+(\omega,z)}{P}$ and $\Phi_{pq}(\omega_i) = \overline{k}_q\overline{x}_p$ (pressure transfer functions from linear wave theory). β^+ calculated from:

$$\beta^+(\omega, z) = \rho g \frac{cosh\ k(z+d)}{cosh\ kd} \tag{5}$$

Now it becomes trivial to substitute the transfer function with transfer functions giving horizontal forces (pressures integrated along a vertical line).

If the P measured surface elevations are filtered through Q linear filters each characterised by gain $H^*_{pq}(\omega_i)$ and phaseshift $\Phi_{pq}(\omega_i)$. Then the sum of the outputs from these $P \cdot Q$ filters is an estimate on the force per meter in $\overline{x} = \overline{0}$, F^*:

$$F^*(t) = \sum_{p=1}^{P}\sum_{q=1}^{Q}\sum_{i=1}^{I}\sum_{j=1}^{J} H^*_{pq}(\omega_i) a_{ij} cos(\omega_i t - \overline{k}_{ij}\overline{x}_p + \phi_{ij} + \Phi_{pq}(\omega_i)) \tag{6}$$

given that $H^*_{pq}(\omega_i) = \frac{\beta^{+,*}(\omega)}{P}$ and $\Phi_{pq}(\omega_i) = \overline{k}_q\overline{x}_p$ (integrated pressure transfer functions from linear wave theory). $\beta^{+,*}$ calculated from:

$$\beta^{+,*}(\omega) = \int_{bottom}^{top} \rho g \frac{cosh\ k(z+d)}{cosh\ kd} dz \tag{7}$$

for cases where integration boundaries are: bottom=-d and top=0 the solution is:

$$\beta^{+,*}(\omega) = \frac{\rho g}{k}\frac{sinh\ kd}{cosh\ kd} \tag{8}$$

for other cases the transfer functions must be calculated numerically.

In the following examples all transfer functions are multiplied by a factor 2 since a reflection coefficient of 100 % is assumed.

5 Results and Discussions

5.1 Measured contra Predicted Pressures

The predicted pressures were found to be in very good agreement with the measured pressures.

This is actually not very surprising because the tested wave conditions corresponds to low wave steepness (non–breaking) where the wave pressures easily can be calculated using the transfer functions from linear wave theory.

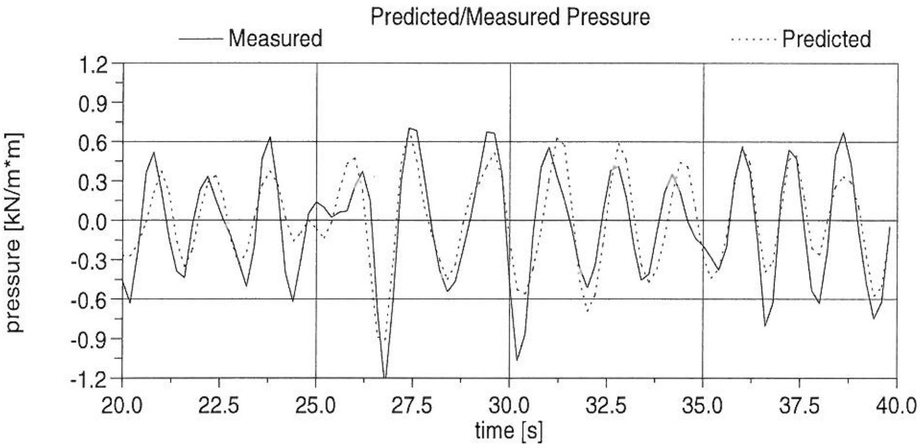

Figure 6: Example of prediction of recorded pressures.

Figure 6 shows a comparison between predicted and measured pressure. The result is from test 017 ($H_S = 0.136m, T_p = 1.5sec., \theta_M = 30\,\text{deg}, \sigma = 15\,\text{deg}$). The pressure cell was situated 0.15 m below still water level. In the prediction of the pressures a reflection coefficient of 1.0 was used.

For the highest peaks the measured pressures are slightly higher than the predicted pressures. This is because linear wave theory starts to fail for these high waves. Nevertheless it is surprising how well linear wave theory predicts the pressures. This might be because the highest pressures are reduced due to much overtopping.

5.2 Measured contra Predicted Wave Forces

Instead of predicting the pressures it is possible to predict the forces per unit length by using the transfer functions from linear wave theory integrated from bottom to still water level or to the actual elevation. As the elevation changes in time it can also be convenient to use heigth of the freeboard as the integration boundary in order to to have a fixed boundary representing the largest forces. This will lead to good estimations of the maximum forces but at the same time to poorer estimates of the forces in the rest of the time series.

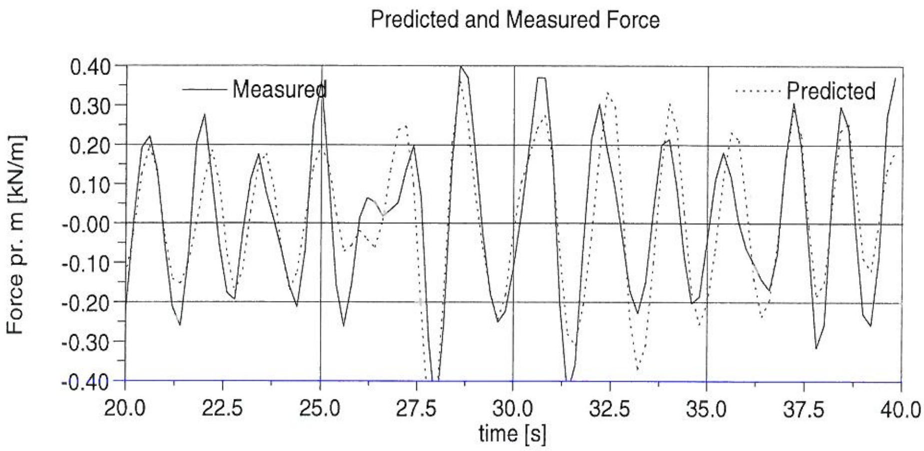

Figure 7: Example of prediction of force.

Figure 7 shows an example of the forces, calculated by integrating the pressures shown in figure 6 to still water level. It is seen that the largest forces are slightly underpredicted.

5.3 Maximum Wave Force per unit length of the caisson as function of the caisson length

Battjes (1982) has considered the effects of short–crestedness of incident waves on the loads on a long structure. His results are expressed as frequency–dependent, directionally–averaged spectral multiplication factors for the load relative to the case of normally, incident, long–crested waves.

All Battjes (1982) results are numerically calculated, and only a short verification was done by comparison with laboratory tests by Traettenberg (1968).

In the present tests, it is found that all Battjes results (multiplication factors) can be used for the calculation of the reduction of the wave forces on the caissons. This is because the wave pressures on the caissons are described with good accuracy by linear wave theory.

The present tests can be seen as a verification of the paper by Battjes.

6 Conclusion

A new method for real time prediction of wave pressures and wave forces has been presented and verified.

The method is able to estimate pressures from short–crested non–breaking waves on vertical walls very accurately. Also time series of forces can be calculated. Consequently the effects of short–crestedness on the wave loads on long caissons can be calculated.

The performed tests clearly verify that already known and commenly used reduction factors for the wave forces are acceptable for use in the case of non–breaking waves.

7 Acknowledgements

This report has been produced as part of a combined LIP–MAST–TAW project. The results are based on experiments carried out at Delft Hydraulics, The Netherlands. All contributers and participants are acknowledged for there cooperation. Also thanks to the technical staff at Delft Hydraulics.

8 References

Battjes, Jurjen A.: Effects of short–crestedness on wave loads on long structures. Applied Ocean Research, 1982, Vol. 4, No. 3.

Helm–Petersen, Jacob: Reflection from Caissons in Multidirectional Seas. Proc. 3rd workshop on Monolithic (Vertical) Coastal Structures, De Voorst, The Netherlands, November 1994.

Traettenberg, A.: The effect of wave crests on wave forces. Proc. 11th Int. Conf. Coastal Eng., London 1968.